Convergence in light transmission properties of transparent wing areas in clearwing mimetic butterflies

Charline Pinna[1$], Maëlle Vilbert[2], Stephan Borensztajn[3], Willy Daney de Marcillac[4], Florence Piron-Prunier[1], Aaron F. Pomerantz[5,6], Nipam Patel[5], Serge Berthier[4], Christine Andraud[2], Doris Gomez[7*], Marianne Elias[1*]

Affiliations:
[1] ISYEB, 45 rue Buffon, CP50, Paris, CNRS, MNHN, Sorbonne Université, EPHE, France
[2] CRC, 36 rue Geoffroy-Saint-Hilaire, CP21, Paris, MNHN, France
[3] IPGP, 1 rue Jussieu, Paris, Université de Paris, CNRS, France
[4] INSP, 4 place Jussieu, boîte courrier 840, Paris, Sorbonne Université, CNRS, France
[5] Marine Biological Laboratory, Woods Hole, Massachusetts, USA
[6] Department Integrative Biology, University of California Berkeley, USA
[7] CEFE, 1919 route de Mende, Montpellier, CNRS, Univ Montpellier, Univ Paul Valéry Montpellier 3, EPHE, IRD, France

*Equal contribution

$ corresponding author: charline.pinna1@edu.mnhn.fr

Abstract

Müllerian mimicry is a positive interspecific interaction, whereby co-occurring defended prey species share a common aposematic signal that advertises their defences to predators. In Lepidoptera, aposematic species typically harbour conspicuous opaque wing colour pattern, which have convergent optical properties, as perceived by predators. Surprisingly, some aposematic mimetic species have partially or totally transparent wings, which raises the question of whether optical properties of such transparent areas are also under selection for convergence. To answer this question and to investigate how transparency is achieved in the first place, we conducted a comparative study of optics and structures of transparent wings in neotropical mimetic clearwing Lepidoptera. We quantified transparency by spectrophotometry and characterised clearwing microstructures and nanostructures by microscopy imaging. We show that transparency is convergent among co-mimics in the eyes of predators, despite a large diversity of underlying micro- and nanostructures. Notably, we reveal that nanostructure density largely influences light transmission. While transparency is primarily produced by

modification of microstructure features, nanostructures may provide a way to fine-tune the degree of transparency. This study calls for a change of paradigm in transparent mimetic lepidoptera: transparency not only enables camouflage but can also be part of aposematic signals.

Significance

Transparency in animals has long been associated to camouflage, but the existence of aposematic mimetic Lepidoptera with partly transparent wings raises the question of the role of transparency in aposematism. Here, we undertake the first comparative analysis of transparency features in mimetic Lepidoptera. We show that transparency is likely part of the aposematic signal, as light transmission properties are convergent among co-mimics. We also reveal a high diversity of wing structures (scales and wing membrane nanostructures) underlying transparency, which enables fine-tuning the degree of transparency. This study, at the interface between physical optics and evolutionary biology, sheds light on the evolution of transparency in aposematic mimetic lineages and may promote bioinspired applications for transparent materials such as antireflective devices.

Introduction

Lepidoptera (butterflies and moths) are characterized by large wings typically covered by scales, as testified by the name of the order (after the ancient greek *lepís* - scale and *pterón* – wing). Scales can contain pigments or generate interferential colours, thereby producing colour patterns across the entire wing. Wing colour patterns are involved in thermoregulation (Dufour et al. 2018; Heidrich et al. 2018), sexual selection (Kemp 2007) and anti-predator defences, such as camouflage (Arias et al. 2019, 2020; Endler 1984), masquerade (Skelhorn et al. 2010; Stoddard 2012), disruptive coloration, and deflection of predator attacks (Stevens, Stubbins, and Hardman 2008). Another type of anti-predator defence in Lepidoptera involving wing colour pattern is aposematism, where the presence of secondary defences is advertised by the means of bright and contrasted colour patterns. Because of the positive frequency-dependent selection incurred on aposematic signals (Greenwood et al. 1989, Chouteau et al. 2016), aposematic species often engage in Müllerian mimetic interactions, whereby species exposed to the same suite of predators converge on the same colour pattern and form mimicry 'rings' (Müller 1879). Co-mimetic

species (species that share a common aposematic colour pattern) are often distantly related, implying that the same colour pattern has evolved independently multiple times. Among such co-mimetic Lepidopteran species, several studies using visual modelling have shown that analogous colour patches (i. e., those occupying a similar position in the wing and harbouring similar colour) cannot be discriminated by birds, believed to be the main predators (Llaurens, Joron, and Théry 2014; Su, Lim, and Kunte 2015; Thurman and Seymoure 2016). Therefore, mimicry selects for convergent colourations, as perceived by predators.

Surprisingly, although most aposematic Lepidoptera species harbour brightly coloured patterns, some unpalatable, aposematic species exhibit transparent wing areas (McClure et al. 2019). In those species, wing colour pattern typically consists in a mosaic of brightly coloured and transparent patches. Notably, in tropical America, many mimicry rings are comprised of such transparent species (Beccaloni 1997; Elias et al. 2008; Willmott et al. 2017). Mimicry among species harbouring transparent patches raises the question of selection for convergence in optical properties, as perceived by predators, in those transparent patches.

A related question is whether transparency in co-mimetic species is achieved by the means of similar structural changes in wings and scales. Previous studies on a handful of species (most of which are not aposematic) have revealed several, non-mutually exclusive means to achieve transparency, through scale modification or scale shedding, with the effect of reducing the total coverage of the chitin membrane by scales. Scales can fall upon adult emergence (Yoshida et al. 1996); they can be reduced (Dushkina, Erten, and Lakhtakia 2017; Perez Goodwyn et al. 2009) and even resemble bristle or hair (Binetti et al. 2009; Hernández-Chavarría, Hernández, and Sittenfeld 2004; Perez Goodwyn et al. 2009; Siddique, Gomard, and Hölscher 2015); they can be either flat on the membrane (Perez Goodwyn et al. 2009) or erected (Dushkina, Erten, and Lakhtakia 2017; Perez Goodwyn et al. 2009), which also reduces effective membrane coverage by scales. Reducing scale density could also make wings transparent to some extent (Perez Goodwyn et al. 2009). Although this has not been reported in transparent lepidoptera, transparent scales, such as those covering coloured scales in the opaque butterfly *Graphium sarpedon* (Stavenga, Giraldo, and Leertouwer 2010), could also be a means to achieve transparency. In addition to scale modifications, the presence of nanostructures on the surface of the wing membrane may enhance transparency through the reduction

of light reflection, by generating a gradient of refractive index between the chitin-made membrane and the air (Binetti et al. 2009; Siddique, Gomard, and Hölscher 2015; Yoshida et al. 1997). Yet, so far, no study has compared the microstructures (scales) and nanostructures present in transparent patches across co-mimetic species. Furthermore, the diversity of structures described above may lead to a range of transparency efficacy. Exploring the link between structural features and optical properties can shed light on whether and how different structures might achieve similar degrees of transparency in the context of mimicry.

Here, we investigate the convergence of transmission properties of transparent areas among co-mimetic butterflies and moths and the structural bases of transparency on 62 Neotropical transparent species, which belong to seven different Lepidoptera families and represent 10 distinct mimicry rings. We characterize wing micro- and nanostructures with digital microscopy and SEM imaging and measure transmission properties of transparent patches using spectrophotometry. We implement comparative analyses that account for phylogenetic relatedness, to (1) examine the putative convergence of transparent patches in visual appearance as seen by bird predators, (2) identify which structures are involved in transparency in the different co-mimetic species and finally (3) explore the links between structural features and transmission properties of transparent patches.

Results & Discussion

Convergence among co-mimics in visual appearance of transparent areas as seen by bird predators

To assess whether transparent areas of co-mimetic species were under selection for convergence due to mimicry, we tested whether these transparent areas, as perceived by predators, were more similar among co-mimetic species than expected at random and given the phylogeny. We used spectrophotometry to measure specular transmittance of the transparent areas, which is a quantitative measurement of transparency. We applied bird vision modelling on the resulting spectra and performed a PERMANOVA and a phylogenetic MANOVA, respectively, on the coordinates in tetrahedral colour space and luminance (which is perceived brightness), setting mimicry ring as factor. The results of

the most ecologically relevant vision models (Lepidoptera viewed against a leaf in forest shade) are presented in Table 1 but the other vision models yield similar results (Supplementary table 1). We show that whether we control for phylogenetic relationship or not, predators see transparent patches among co-mimetic species as more similar than among species that belong to different mimicry rings, mirroring what has been shown for coloured patches in opaque species (Llaurens, Joron, and Théry 2014; Su, Lim, and Kunte 2015; Thurman and Seymoure 2016). The fact that the test remains significant with the phylogenetic correction indicates that such similarity in transparent patches is due to convergent evolution. When investigating separately the effects of achromatic aspects (luminance) and chromatic aspects (tetrahedral coordinates x, y and z), the former appear more significant than the latter (Table 1), suggesting that selection may act more on mean transmittance (degree of transparency) than on colour. Overall, our results suggest that, for mimetic Lepidoptera, transparent areas, especially the degree of transparency, are under selection for convergence and are therefore part of the aposematic signal.

Diversity of structures involved in transparency

Convergence in transmission among co-mimetic species raises the question of the nature and similarity of clearwing micro- and nanostructures among co-mimetic species. We therefore explored the diversity of structures present in the transparent patches in the 62 species. We used digital photonic microscopy and SEM imaging to characterize the structures present in the transparent zones (type, insertion, colour, length, width, and density of scales; type and density of nanostructures; wing membrane thickness).

We find a diversity of microstructural features in transparent areas (Figure 1A). Scales can be coloured (76% of species) or transparent (24%); they can be flat on the membrane (16%) or erected (84%). Scales can be 'standard' (i. e., a two-dimension structure, 55% of species), or hair-like (45%). Forked hair-like scales have been reported in the highly transparent nymphalid species *Greta oto* (Binetti et al. 2009; Siddique, Gomard, and Hölscher 2015), which belongs to the mimetic butterfly Ithomiini tribe. In our dataset, hair-like scales appear to be almost exclusively found in the Ithomiini tribe, although one erebid species also harbours bristle-like scales. Erected scales (*i. e.,* with a non-flat angle between the scale basis and the wing membrane) have been previously reported in the riodinid *Chorinea sylphina* (Dushkina, Erten, and Lakhtakia 2017) and in the nymphalid *Parantica sita* (Perez Goodwyn et al. 2009). Here we describe, as Gomez et al. (2020, in

review) did for the first time, some species with coloured erected scales that are completely perpendicular to the wing membrane, such as in the ithomiine *Methona curvifascia*. Transparent scales have already been reported in the opaque papilionid *Graphium sarpedon* (Stavenga, Giraldo, and Leertouwer 2010) and as Gomez et al (2020, in review) we are describing them for the first time in transparent Lepidoptera. Other means of achieving transparency reported in the literature are not observed among our species (e. g., wing membrane devoid of scales, Yoshida et al. 1996). However, our study is restricted to mimetic transparent butterflies and, as such, spans a relatively small number of families. An exhaustive study on all families comprising species with partially or totally transparent wings is needed to investigate thoroughly the different structures that might be involved in transparency.

We also reveal an unexpected diversity of nanostructures covering wing membrane (Figure 1B). In our sample, we find five types of nanostructures: absent (10% of species), maze (3%), nipple arrays (55%), pillars (21%), and moss (11%). While nipple arrays and pillars have previously been described on the wing of the sphingid *Cephonodes hylas* (Yoshida et al. 1997) and in the nymphalid *G. oto* (Binetti et al. 2009; Siddique, Gomard, and Hölscher 2015), respectively, maze-like nanostructures have only been reported on the corneal surface of insect eyes (Blagodatski et al. 2015). Similarly, the moss type of nanostructures is reported here for the first time. Those nanostructures can be related to the classification proposed by Blagodatski et al. (2015): pillars are a subcategory of nipple arrays, with higher and more densely packed nipples with an enlarged basis; moss-like nanostructures are similar to dimples (holes embedded in a matrix), although with much bigger and more profound holes. Nipples, mazes and dimples have been found to be produced by Turing's reaction-diffusion models, a solid framework that explains pattern formation in biology (Turing 1952). While the principle of formation can be elegantly modelled, developmental studies are needed to understand the process by which nanostructures are laid on butterfly wing membrane.

Phylogenetic signal tests show that both micro- and nanostructure features are highly conserved in the phylogeny (Figure 2, Supplementary Table 2), suggesting the existence of constraints in the developmental pathways underlying micro- and nanostructures. However, in the nymphalid tribe Ithomiini, which is highly represented is our dataset, microstructures seem to be more conserved (all species but the basal species *M.*

curvifascia only have hair-like scales in transparent areas) than nanostructures (all five types of nanostructures, mixed in the Ithomiini clade).

There is a significant association between mimicry rings and structural features (Fischer exact test on scale type and insertion and mimicry rings: p-value < 0.001 and Fischer exact test on nanostructure type and mimicry ring: p-value < 0.001), meaning that in some mimicry rings one type of micro- or nanostructures is more represented than in other mimicry rings (Supplementary figure 1). For example, in the 'panthyale' and 'theudelinda' mimicry rings, species have only hair-like scales and mostly pillar nanostructures. In the 'confusa' mimicry ring, species often harbour erected scales (five out of seven species) and do not have any nanostructure covering their wing membrane (six out of seven species). These associations may be either the result of common ancestry or the result of convergence. For the 'panthyale' and 'theudelinda' mimicry rings, as species tend to be closely related, their structures are likely inherited from a common ancestor. For the 'confusa' mimicry ring, however, species are distantly related, suggesting evolutionary convergence, even though we cannot rule out that the absence of nanostructures may be ancestral and inherited from a common ancestor. Although different structures can be involved in transparency for each mimicry ring, the structures in transparent areas of co-mimetic species tend to be similar, and likely convergent in some cases.

Mimicry rings are characterized by transmission properties of transparent areas, mainly the degree of transparency, which is under selection for convergence. Are some structures independently selected in different species belonging to some mimicry rings because they confer a peculiar visual aspect, typical of the mimicry ring, and therefore participating in the aposematic signal? This raises the question of the link between transmission properties and structures in the transparent areas.

Link between structural features and transmission properties

To investigate whether transmission properties depend on the structures present in the transparent zones we measured the specular transmittance of transparent areas of each species with a goniospectrophotometer and we calculated the mean transmittance over 300-700nm, hereafter called mean transmittance, for each spectrum. We first confirmed that the physical property 'mean transmittance' (a proxy for the degree of transparency), is correlated to what is perceived by predators (the x, y and z coordinates and luminance

from visual models) performing a mixed linear model and a Phylogenetic Generalized Least Square (PGLS) analysis (see Supplementary result 1 for details). Across the 62 species, mean transmittance ranges from 0.0284% in *Eresia nauplius* to 71.7% in *Godyris panthyale* (mean: 29.2%, median: 31.6%, supplementary table 3). We performed Phylogenetic Generalized Least Squares (PGLS) to assess the relationship between mean transmittance and micro- and nanostructural features (type, insertion, colour, length, width and density of scales; type and density of nanostructures; wing membrane thickness; including some interactions), while accounting for phylogeny. We retained as best models all models within 2 AICc units of the minimal AICc value. Following this procedure, eight models were retained.

Mean transmittance depends mainly on scale type, scale density and nanostructure density, and to a lesser extent on membrane thickness and scale colour (Table 2, Supplementary table 4). The effect of scale type and insertion is retained in all eight models and is significant in all of them. Wings covered with hair-like scales transmit more light than those covered with standard scales (Figure 3A). Among wings covered with standard scales, those with erected scales transmit more light than those with flat scales. The effect of scale density is retained in the eight best models and is significant in five of those (Supplementary table 4): mean transmittance decreases as scale density increases. Mean transmittance thus increases when membrane coverage decreases (due to reduced scale surface and/or scale density), because there is less material interacting (reflecting, diffusing, or absorbing) with light. The effect of nanostructure density is retained in six models and is significant in four of those: mean transmittance increases when nanostructure density increases (Figure 3B). Light transmission is negatively correlated to light reflection and nanostructures are known to have anti-reflective properties, as demonstrated in the sphingid *Cephonodes hylas* (Yoshida et al. 1997) and in the nymphalid *G. oto* (Siddique, Gomard, and Hölscher 2015). Reflection increases as the difference in refractive index between air and organic materials increases. Nanostructures create a gradient of refractive index between air and wing tissue, and gradient effectiveness in reducing reflection increases with gradient progressiveness. For instance, pillars with conical basis are more effective at cancelling reflection than cylinders because cones produce a smoother air:chitin gradient from air to wing than cylinders (Siddique, Gomard, and Hölscher 2015). Nanostructure shape is thus important in creating a smooth gradient. In our case, nanostructure density is highly correlated to

nanostructure type, which we have defined according to their shape (phylogenetic ANOVA on nanostructure density with nanostructure type as factor: F = 26.26, p-value = 0.001, see supplementary result 2 for details): the nanostructures whose shape likely creates the smoother gradient (pillar and moss) are also the denser ones. When nanostructure density increases, light reflection thus decreases. Light can either be transmitted, reflected or absorbed, and assuming that the chitin wing membrane only absorbs a small amount of light between 300 and 700 nm (Stavenga et al. 2014), when light reflection decreases, due to the presence of nanostructures, light transmission necessarily increases, which explains the positive effect of nanostructure density on mean transmittance.

The interaction between scale density and nanostructure density is retained in three out of eight models and it is marginally significantly different from zero in two of those three models (supplementary table 4). The coefficient is always negative, meaning that the increase in light transmission due to the increase in nanostructure density is not as strong when scale density is high than when scale density is low. This suggests that the contribution of nanostructures to transparency is stronger when scale density is low. Selection can act on microstructures (scales) and nanostructures. As nanostructures seem more labile than microstructures and allow fine-tuning of transparency, they could therefore evolve more readily in response to selection on the degree of transparency. The interplay between scales and nanostructures can thus modulate the degree of transparency.

The effect of membrane thickness is retained in three out of eight models and is significantly different from zero in one of them: light transmission decreases when membrane thickness increases. Wing membrane is mainly made of chitin and given that chitin absorbs a little amount of light (Stavenga et al. 2014), thicker membranes, which contain more chitin, absorb more light than thinner ones, thereby reducing light transmission.

Transparent scales, which do not contain pigments, transmit more light than coloured ones, which contain pigments; a relationship which is retained in three out of eight models and is marginally significantly different from zero in one model (supplementary table 4). Pigments, such as melanin or ommochrome commonly found in butterfly scales, absorb some part of the light spectrum, thereby reducing light transmission.

Other variables that were included in the model (scale length and width, nanostructure type, the interaction between scale type and scale density and the triple interaction between scale length, width and density) are not retained in any models (Supplementary table 4). These results suggest that those variables might not have any effect on transparency.

While we show a high structural diversity, future studies should thoroughly quantify the relative contributions of micro and nanostructures on the produced optical effects, notably on reflection in transparent areas.

Conclusion

Our comparative analysis on transparent mimetic Lepidoptera showed that the transmission properties of transparent wing areas are convergent between co-mimetic species, suggesting that visual features of transparent areas are part of the aposematic signal. Despite an unexpected diversity of micro- and nanostructures underlying transparency, these structures are more similar than expected at random among co-mimetic species, perhaps because they confer typical visual aspects that are characteristic of the aposematic signal of the different mimicry rings. The diversity of nanostructures described may encourage bio-inspired applications for transparent materials.

This study challenges our vision on transparency, which might have evolved under multiple selective pressures in aposematic butterflies. Transparency has been shown to be involved in camouflage and to decrease detectability by predators (Arias et al. 2020), even in aposematic species (Arias et al. 2019). Nevertheless, our results suggest that transparent patches participate in the aposematic signal and that selection acts on the transmission properties of these patches, mainly on the degree of transparency but also on chromatic aspects. Therefore, transparent aposematic Lepidoptera benefit from a double protection from predation, which can act at different distances (Barnett et al. 2018; Cuthill 2019; Tullberg, Merilaita, and Wiklund 2005). Transparent aposematic species are less detectable than opaque species, but when detected they may be recognized as an unpalatable prey due to their aposematic signal. However, transparency entails strong structural modifications of scales that might impair other functions such as thermoregulation (Berthier 2005) or hydrophobicity (Perez Goodwyn et al. 2009). Transparency may therefore come at a cost in those large-winged insects, which may explain why it is not pervasive among Lepidoptera.

Materials & Methods

Material

In this study, we focus on 62 different species represented by 1 or 2 specimens collected with hand nets in understory forests in Peru and Ecuador by ourselves and private collectors (Supplementary table 5). They belong to 7 different families (Nymphalidae, Riodinidae, Pieridae, Papilionidae, Erebidae, Notodontidae, Geometridae) and represent 10 different mimicry rings, following the classification used in Ithomiini: 'agnosia', 'aureliana', 'banjana-m', 'confusa', 'eurimedia', 'hewitsoni', 'lerida', 'panthyale', 'theudelinda' (Chazot et al. 2014; Willmott et al. 2017; Willmott and Mallet 2004). In addition, we call 'blue' a mimicry ring that does not include Ithomiini species.

Phylogeny

We used both published and *de novo* sequences from one mitochondrial gene and seven nuclear genes, representing a total length of 7433 bp to infer a molecular phylogeny. To improve the phylogeny topology, we added 35 species representing 8 additional families to the dataset (see Supplementary table 5 and SI). We performed a Bayesian inference of the phylogeny using BEAST 1.8.3. We forced the monophyly of some groups and we added eleven secondary calibration points (see Supplementary table 6) according to Kawahara et al. (2019).

Spectrophotometry

Specular transmittance was measured over 300-700 nm, a range to which both birds and butterflies are sensitive (Briscoe and Chittka 2001; Hart 2001) using a home-built goniospectrophotometer (see SI for details). For each species, we measured five different spots in the transparent areas on the ventral side of the forewing. We computed mean transmittance over 300-700 nm from smoothen spectra using Pavo2 (Maia et al. 2019), as a proxy for transparency: wing transparency increases as mean transmittance increases. We ensured that all measurements were repeatable (see SI), and we considered that any individual is representative of its species. One specimen per species was therefore used in most subsequent analyses.

High-resolution imaging and structure characterization

We observed structures with a digital photonic microscope (Keyence VHX-5000) to

367 determine scale type (standard scale vs. hair-like scale), scale colour (coloured vs.
368 transparent) and scale insertion (flat vs. erected) on ventral side. Wings were imaged in
369 SEM (Zeiss Auriga 40) to measure scale density, scale length and width, membrane
370 thickness, and nanostructure density (see SI for more details). As scale structural features
371 were shown to be repeatable (see SI) within species we used one specimen per species.
372
373 *Vision models*
374 We used bird vision modelling on the smoothened transmission spectra to test whether
375 transparent areas of comimetic species are perceived as similar by birds. Birds differ in
376 their sensitivity to UV wavelength: some are more sensitive to UV (UVS vision) than others
377 (VS vision). As predators of neotropical butterflies can belong to either category
378 (Dell'Aglio et al. 2018), we used *Puffinus pacificus* as a model for VS vision and *Cyanistes*
379 *caeruleus* as model for UVS vision. We considered different light environments differing
380 in their intensity and spectral distribution: forest shade, woodland shade and large gap as
381 defined by Endler (1993). We also considered different viewing conditions: the
382 transparent patch of the butterfly could be seen against the sky (light is just transmitted
383 through the wing) or it could be seen against a leaf (light is transmitted through the wing,
384 then reflected on the leaf and transmitted again through the wing). In total we calculated
385 12 different vision models, using R package Pavo 2 (Maia et al. 2019), depending on the
386 different combinations of bird visual system, light environment and viewing conditions.
387 We extracted the x, y and z coordinates in the tetrahedral colour space corresponding to
388 each smoothened spectrum in each vision model and the luminance (which corresponds
389 to perceived brightness).
390
391 *Statistical analyses*
392 All statistical analyses were performed with the software R version 3.6.2. (R Core Team
393 2019).
394 *Convergence on optical properties*
395 To assess whether transparent areas, as perceived by predators, were more similar than
396 expected at random and convergent among co-mimetic species, we performed a non-
397 parametric PERMANOVA (with the R package 'vegan' (Oksanen et al. 2019)) and a
398 phylogenetic MANOVA (which accounts for species relatedness with the R package
399 'geiger' (Pennell et al. 2014)) on the mean of each coordinate in the tetrahedral colour

space and the luminance (i.e. the perceived brightness) across the five spots measured (except for species belonging to the mimicry ring 'agnosia' where we excluded the spot in white band), with mimicry ring as the explanatory variable. To disentangle the effect of chromatic aspects (x, y and z coordinates) and achromatic aspects (luminance), we also performed a Kruskal-Wallis test and a phylogenetic ANOVA implemented in the R package 'phytools' (Revell 2012) on luminance and a PERMANOVA and a phylogenetic MANOVA on the coordinates x, y and z with mimicry ring as factor, as described above.

Phylogenetic signal

To assess whether transmission properties and structural features were conserved in the phylogeny, we estimated the phylogenetic signal of each variable. For quantitative variable (mean transmittance, scale density, scale length, scale width, nanostructure density and membrane thickness), we calculated both Pagel's λ (Pagel 1999) and Blomberg's K (Blomberg, Garland, and Ives 2003) implemented in the R package 'phytools' (Revell 2012). For multicategorical variables (scale type and nanostructure type), we used the delta statistic (Borges et al. 2019) and we compared it to the distribution of values of delta when the trait is randomised along the phylogeny to estimate whether the trait is randomly distributed along the phylogeny. Finally, for binary variables (scale colour), we used Fritz and Purvis' D (Fritz and Purvis 2010) implemented in the R package 'caper' (Orme et al. 2018).

Association between structures and mimicry ring

We tested whether there was an association between some structure type (scale type and nanostructure type) and mimicry ring by performing Fisher's exact.

Link between transparency (mean transmittance) and structures

To assess the link between structural features and the degree of transparency we only used the spectrophotometric data of the points that correspond to the location of the SEM images (between 1 and 3 points per species) and we calculated the average of mean transmittance over 300-700 nm for each specimen. We tested the link between this average mean transmittance and all the structural features we measured (scale type, scale colour, scale density, scale length, scale width, nanostructure type, nanostructure density, membrane thickness and the following interactions: interaction between scale type and

scale density, interaction between scale density and nanostructure density and the triple interaction between scale density, scale length and scale width) while controlling for phylogenetic relationships by performing pgls implemented in the R package 'caper' (Orme et al. 2018). We compared all possible models with all the structural variables, but we prevented some variables from being in the same model because they were highly correlated, using the R package 'MuMIn' (Barton 2019). Among the 308 models, we selected the best models (difference in AICc inferior to 2). Eight such models were retained.

Acknowledgments/funding

We thank Jonathan Pairraire and Céline Houssin for the help with photonic imaging and Josquin Gerber and Edgar Attivissimo for spectroscopic measurements. We thank Benoit Vincent for the identification of some Arctiini specimens. We are thankful to the Institut de Physique du Globe de Paris (IPGP) for giving us access to SEM and to the Peruvian and Ecuadorian governmental authorities for collection permits (021C/C-2005-INRENA-IANP, 002-2015-SERFOR-DGGSPFFS, 373-2017-SERFOR-DGGSPFFS, 005-IC-FAU-DNBAPVS/MA, 019-IC-FAU-DNBAPVS/MA). This work was funded by Clearwing ANR project (ANR-16-CE02-0012), HFSP project on transparency (RGP0014/2016) and a France-Berkeley fund grant (FBF #2015--58).

References

Arias, Mónica et al. 2019. "Transparency Reduces Predator Detection in Mimetic Clearwing Butterflies." *Functional Ecology* 33(6): 1110–19.

———. 2020. "Transparency Improves Concealment in Cryptically Coloured Moths." *Journal of Evolutionary Biology* 33(2): 247–52.

Barnett, James B, Constantine Michalis, Nicholas E Scott-Samuel, and Innes C Cuthill. 2018. "Distance-Dependent Defensive Coloration in the Poison Frog Dendrobates Tinctorius, Dendrobatidae." *Proceedings of the National Academy of Sciences of the United States of America* 115(25): 6416–21. http://www.ncbi.nlm.nih.gov/pubmed/29866847 (April 24, 2020).

Barton, Kamil. 2019. "MuMIn: Multi-Model Inference." https://cran.r-project.org/package=MuMIn.

Beccaloni, George W. 1997. "Ecology , Natural History and Behaviour of Ithomiine

Butterflies and Their Mimics in Ecuador (Lepidoptera : Nymphalidae : Ithomiinae)." *Tropical Lepidoptera* 8(2): 103–24.

Berthier, S. 2005. "Thermoregulation and Spectral Selectivity of the Tropical Butterfly Prepona Meander: A Remarkable Example of Temperature Auto-Regulation." *Applied Physics A: Materials Science and Processing* 80(7): 1397–1400.

Binetti, Valerie R. et al. 2009. "The Natural Transparency and Piezoelectric Response of the Greta Oto Butterfly Wing." *Integrative Biology* 1(4): 324–29.

Blagodatski, Artem et al. 2015. "Diverse Set of Turing Nanopatterns Coat Corneae across Insect Lineages." *Proceedings of the National Academy of Sciences* 112(34): 10750–55.

Blomberg, Simon P., Theodore Garland, and Anthony R. Ives. 2003. "Testing for Phylogenetic Signal in Comparative Data: Behavioral Traits Are More Labile." *Evolution* 57(4): 717–45.

Borges, Rui et al. 2019. "Measuring Phylogenetic Signal between Categorical Traits and Phylogenies." *Bioinformatics* 35(11): 1862–69.

Briscoe, Adriana D, and Lars Chittka. 2001. "The Evolution of Color Vision in Insects." *Annual Review of Entomology* 46: 471–510. www.annualreviews.org.

Chazot, Nicolas et al. 2014. "Mutualistic Mimicry and Filtering by Altitude Shape the Structure of Andean Butterfly Communities." *The American Naturalist* 183(1): 26–39. http://www.journals.uchicago.edu/doi/10.1086/674100.

Cuthill, I. C. 2019. "Camouflage." *Journal of Zoology* 308(2): 75–92.

Dell'Aglio, Denise Dalbosco et al. 2018. "The Appearance of Mimetic Heliconius Butterflies to Predators and Conspecifics." *Evolution* 72(10): 2156–66.

Dufour, Pauline C. et al. 2018. "Divergent Melanism Strategies in Andean Butterfly Communities Structure Diversity Patterns and Climate Responses." *Journal of Biogeography* 45(11): 2471–82.

Dushkina, Natalia, Sema Erten, and Akhlesh Lakhtakia. 2017. "Coloration and Structure of the Wings of Chorinea Sylphina Bates." *Journal of the Lepidopterists' Society* 71(1): 1–11.

Elias, Marianne, Zachariah Gompert, Chris Jiggins, and Keith Willmott. 2008. "Mutualistic Interactions Drive Ecological Niche Convergence in a Diverse Butterfly Community." *PLoS biology* 6(12): 1–8.

Endler, John A. 1993. "The Color of Light in Forests and Its Implications." *Ecological*

Monographs 63(1): 1–27.

Endler, John A. 1984. "Progressive Background Matching in Moths, and a Quantitative Measure of Crypsis." *Biological Journal of the Linnean Sociey* 22: 187–231.

Fritz, Susanne A., and Andy Purvis. 2010. "Selectivity in Mammalian Extinction Risk and Threat Types: A New Measure of Phylogenetic Signal Strength in Binary Traits." *Conservation Biology* 24(4): 1042–51.

Gomez, D. et al. 2020. "Transparency in Butterflies and Moths: Structural Diversity, Optical Properties and Ecological Relevance." *bioRxiv*: 2020.05.14.093450. https://www.biorxiv.org/content/10.1101/2020.05.14.093450v1 (June 24, 2020).

Greenwood, Jeremy J.D., Peter A. Cotton, Duncan Wilson, and M. 1989. "Frequency-dependent Selection on Aposematic Prey: Some Experiments." *Biological Journal of the Linnean Society* 36(1–2): 213–26.

Hart, Nathan S. 2001. "The Visual Ecology of Avian Photoreceptors." *Progress in Retinal and Eye Research* 20(5): 675–703.

Heidrich, Lea et al. 2018. "The Dark Side of Lepidoptera: Colour Lightness of Geometrid Moths Decreases with Increasing Latitude." *Global Ecology and Biogeography* 27(4): 407–16.

Hernández-Chavarría, Francisco, Alejandro Hernández, and Ana Sittenfeld. 2004. "The 'Windows', Scales, and Bristles of the Tropical Moth Rothschildia Lebeau (Lepidoptera: Saturniidae)." *Revista de Biologia Tropical* 52(4): 919–26.

Kawahara, Akito Y. et al. 2019. "Phylogenomics Reveals the Evolutionary Timing and Pattern of Butterflies and Moths." *Proceedings of the National Academy of Sciences* 116(45): 22657–63. https://www.pnas.org/content/116/45/22657 (March 6, 2020).

Kemp, Darrell J. 2007. "Female Butterflies Prefer Males Bearing Bright Iridescent Ornamentation." *Proceedings of the Royal Society B: Biological Sciences* 274(1613): 1043–47.

Llaurens, V., M. Joron, and M. Théry. 2014. "Cryptic Differences in Colour among Müllerian Mimics: How Can the Visual Capacities of Predators and Prey Shape the Evolution of Wing Colours?" *Journal of Evolutionary Biology* 27(3): 531–40.

Maia, Rafael, Hugo Gruson, John A. Endler, and Thomas E. White. 2019. "Pavo 2: New Tools for the Spectral and Spatial Analysis of Colour in R." *Methods in Ecology and Evolution* 10(7): 1097–1107.

McClure, Melanie et al. 2019. "Why Has Transparency Evolved in Aposematic Butterflies? Insights from the Largest Radiation of Aposematic Butterflies, the Ithomiini." *Proceedings of the Royal Society B: Biological Sciences* 286(1901): 1–10.

Müller, Fritz. 1879. "Ituna and Thyridia : A Remarkable Case of Mimicry in Butterflies." *Kosmos*.

Oksanen, Jari et al. 2019. "Vegan: Community Ecology Packagevegan: Community Ecology Package." https://cran.r-project.org/package=vegan.

Orme, David et al. 2018. "Caper: Comparative Analyses of Phylogenetics and Evolution in R." https://cran.r-project.org/package=caper.

Pagel, M. 1999. "Inferring the Historical Patterns of Biological Evolution." *Nature* 401(6756): 877–84.

Pennell, Matthew W et al. 2014. "Geiger v2.0: An Expanded Suite of Methods for Fitting Macroevolutionary Models to Phylogenetic Trees." *BIOINFORMATICS APPLICATIONS* 30(15): 2216–18. http://github.com/mwpen- (April 27, 2020).

Perez Goodwyn, Pablo, Yasunori Maezono, Naoe Hosoda, and Kenji Fujisaki. 2009. "Waterproof and Translucent Wings at the Same Time: Problems and Solutions in Butterflies." *Naturwissenschaften* 96(7): 781–87.

R Core Team. 2019. "R: A Language and Environment for Statistical Computing." https://www.r-project.org/.

Revell, Liam J. 2012. "Phytools: An R Package for Phylogenetic Comparative Biology (and Other Things)." *Methods in Ecology and Evolution* 3: 217–23.

Siddique, Radwanul Hasan, Guillaume Gomard, and Hendrik Hölscher. 2015. "The Role of Random Nanostructures for the Omnidirectional Anti-Reflection Properties of the Glasswing Butterfly." *Nature Communications* 6: 1–8.

Skelhorn, John, Hannah M. Rowland, Michael P. Speed, and Graeme D. Ruxton. 2010. "Masquerade: Camouflage without Crypsis." *Science* 327(5961): 51.

Stavenga, Doekele G., Marco A. Giraldo, and Hein L. Leertouwer. 2010. "Butterfly Wing Colors: Glass Scales of Graphium Sarpedon Cause Polarized Iridescence and Enhance Blue/Green Pigment Coloration of the Wing Membrane." *Journal of Experimental Biology* 213(10): 1731–39.

Stavenga, Doekele G, · Hein, L Leertouwer, and Bodo D Wilts. 2014. "The Colouration Toolkit of the Pipevine Swallowtail Butterfly, Battus Philenor: Thin Films, Papiliochromes, and Melanin." *J Comp Physiol A* 200: 547–61.

565 Stevens, Martin, Claire L. Stubbins, and Chloe J. Hardman. 2008. "The Anti-Predator
566 Function of 'eyespots' on Camouflaged and Conspicuous Prey." *Behavioral Ecology*
567 *and Sociobiology* 62(11): 1787–93.
568 Stoddard, Mary Caswell. 2012. 58 Current Zoology *Mimicry and Masquerade from the*
569 *Avian Visual Perspec-Tive*. https://academic.oup.com/cz/article-
570 abstract/58/4/630/1787096.
571 Su, Shiyu, Matthew Lim, and Krushnamegh Kunte. 2015. "Prey from the Eyes of
572 Predators: Color Discriminability of Aposematic and Mimetic Butterflies from an
573 Avian Visual Perspective." *Evolution* 69(11): 2985–94.
574 Thurman, T. J., and B. M. Seymoure. 2016. "A Bird's Eye View of Two Mimetic Tropical
575 Butterflies: Coloration Matches Predator's Sensitivity." *Journal of Zoology* 298(3):
576 159–68.
577 Tullberg, Birgitta S., Sami Merilaita, and Christer Wiklund. 2005. "Aposematism and
578 Crypsis Combined as a Result of Distance Dependence: Functional Versatility of the
579 Colour Pattern in the Swallowtail Butterfly Larva." *Proceedings of the Royal Society*
580 *B: Biological Sciences* 272: 1315–21.
581 Turing, A. M. 1952. "The Chemical Basis of Morphogenesis." *Philosophical Transactions of*
582 *the Royal Society of London. Series B, Biological Sciences* 237(641): 37–72.
583 Willmott, Keith R., and James Mallet. 2004. "Correlations between Adult Mimicry and
584 Larval Host Plants in Ithomiine Butterflies." *Proceedings of the Royal Society B:*
585 *Biological Sciences* 271(SUPPL. 5): 266–69.
586 Willmott, Keith R., Julia C. Robinson Willmott, Marianne Elias, and Chris D. Jiggins. 2017.
587 "Maintaining Mimicry Diversity: Optimal Warning Colour Patterns Differ among
588 Microhabitats in Amazonian Clearwing Butterflies." *Proceedings of the Royal Society*
589 *B: Biological Sciences* 284(1855): 1–9.
590 Yoshida, Akihiro, Mayumi Motoyama, Akinori Kosaku, and Kiyoshi Miyamoto. 1996.
591 "Nanoprotuberance Array in the Transparent Wing of a Hawkmoth, Cephonodes
592 Hylas." *Zoological Science* 13(4): 525–26.
593 ———. 1997. "Antireflective Nanoprotuberance Array in the Transparent Wing of a
594 Hawkmoth, Cephonodes Hylas." *Zoological Science* 14(4): 737–41. i0289-0003-13-
595 4-525.pdf.
596

Table 1. Tests of convergence of transparent areas, as perceived by predators, among co-mimetic species

Dependent variable	test	visual system	Statistic	p-value	
xyzL	PERMANOVA	VS	$F_9 = 6.93$	0.001	***
		UVS	$F_9 = 6.88$	0.001	***
	phylogenetic MANOVA	VS	approx-$F_9 = 3.05$	< 0.001	***
		UVS	approx-$F_9 = 2.97$	< 0.001	***
xyz	PERMANOVA	VS	$F_9 = 2.47$	0.021	*
		UVS	$F_9 = 2.52$	0.029	*
	phylogenetic MANOVA	VS	approx-$F_9 = 2.11$	0.063	·
		UVS	approx-$F_9 = 2.04$	0.074	·
L	Kruskal Wallis	VS	$X_9 = 30.9$	< 0.001	***
		UVS	$X_9 = 31.1$	< 0.001	***
	phylogenetic ANOVA	VS	$F_9 = 7.26$	0.001	***
		UVS	$F_9 = 7.26$	0.002	**

Results of the PERMANOVA, phylogenetic MANOVA, Kruskal Wallis test and phylogenetic ANOVA to test the effect of mimicry rings on predator perception of wing transparent areas. Variables x, y and z are the mean coordinates in the tetrahedral colour space of transparent areas for each species and L is the mean luminance. For phylogenetic analyses, p-value is calculated based on simulations. Results shown are those obtained under the most ecologically relevant vision models (forest shade illuminant and Lepidoptera viewed against a leaf).

Table 2. Link between structural features and mean transmittance over 300-700nm.

Structural features	Estimate	Std.Error	t value	p-value	
Mean nanostructure density	1.078	0.383	2.815	0.006712	**
Mean scale density	-0.006339	0.008515	-0.7444	0.4597	
Scale type and insertion Hair vs. Scale	6.898	1.513	4.560	< 0.001	***
Scale type and insertion Flat scale vs. Erected scale	6.67	1.987	3.357	0.001423	**
Interaction between nanostructure density and scale density	-0.001357	0.0007831	-1.732	0.08875	.

Results of the best PGLS model ($F_{5,56}$ = 26.65 (p-value <0.001 ***), AICc = 469.9, R_{adj}^2 = 0.678, λ = 0 (p-value < 0.001 ***)) linking mean transmittance and micro- and nanostructure features.

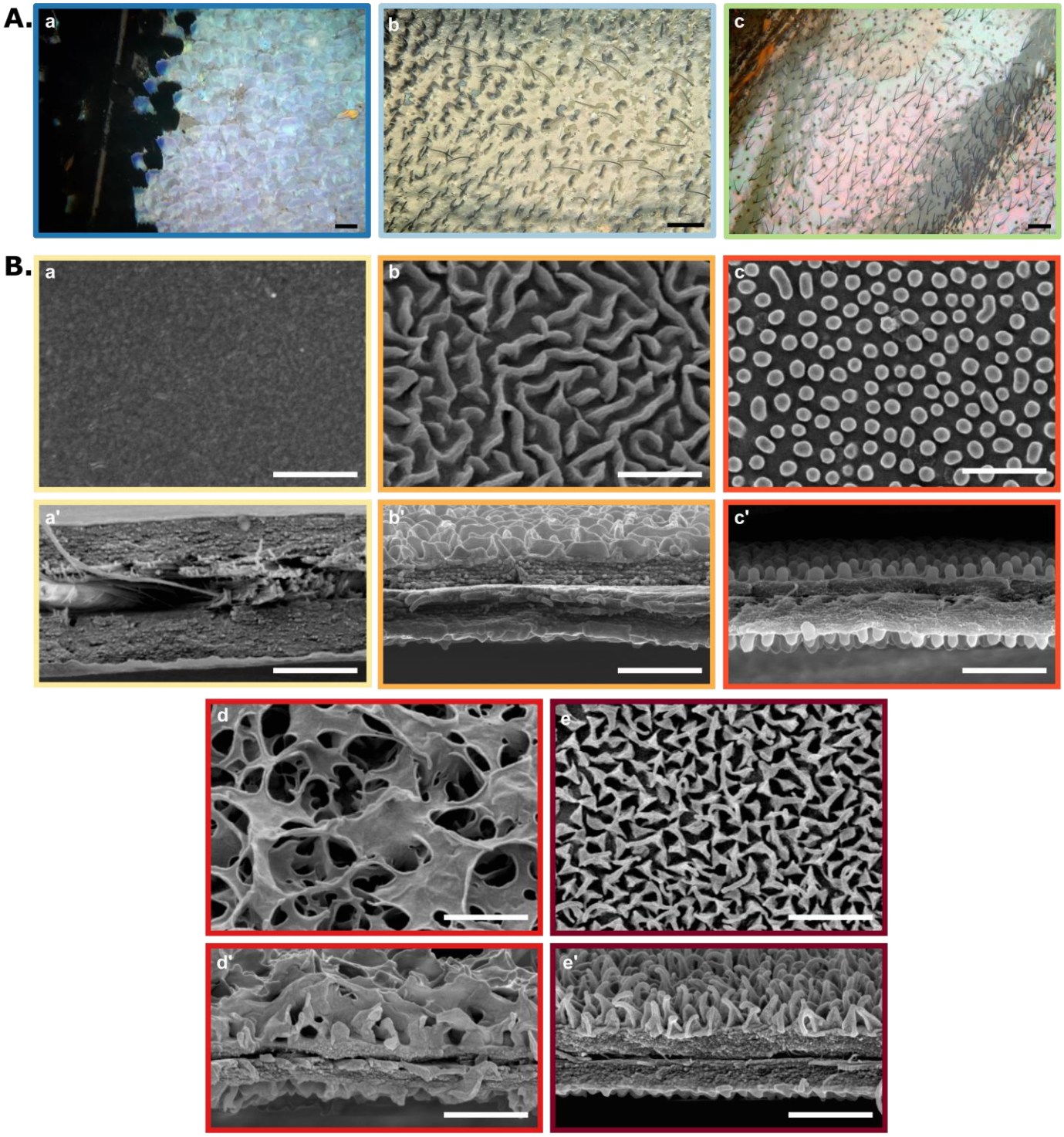

Figure 1. Diversity of micro- and nanostructures involved in transparency.
A. Diversity of microstructures. a. transparent scales of *Hypocrita strigifera,* b. erected scales of *Methona curvifascia* and c. hair-like scales of *Hypomenitis ortygia*. Scale bars represent 100 µm.
B. Diversity of nanostructures. a, b, c, d and e represent topviews and a', b', c', d' and e' represent cross section of wing membrane. Scale bars represent 1 µm. a, a'. absence of nanostructure in *Methona curvifascia*; b, b'. maze nanostructures of *Megoleria orestilla*; c, c'. nipple nanostructures of *Ithomiola floralis*; d, d'. moss nanostructures of *Oleria onega*; e, e'. pillar nanostructures of *Hypomenitis enigma*. Each coloured frame corresponds to a scale type or nanostructure type, as defined in figure 2.

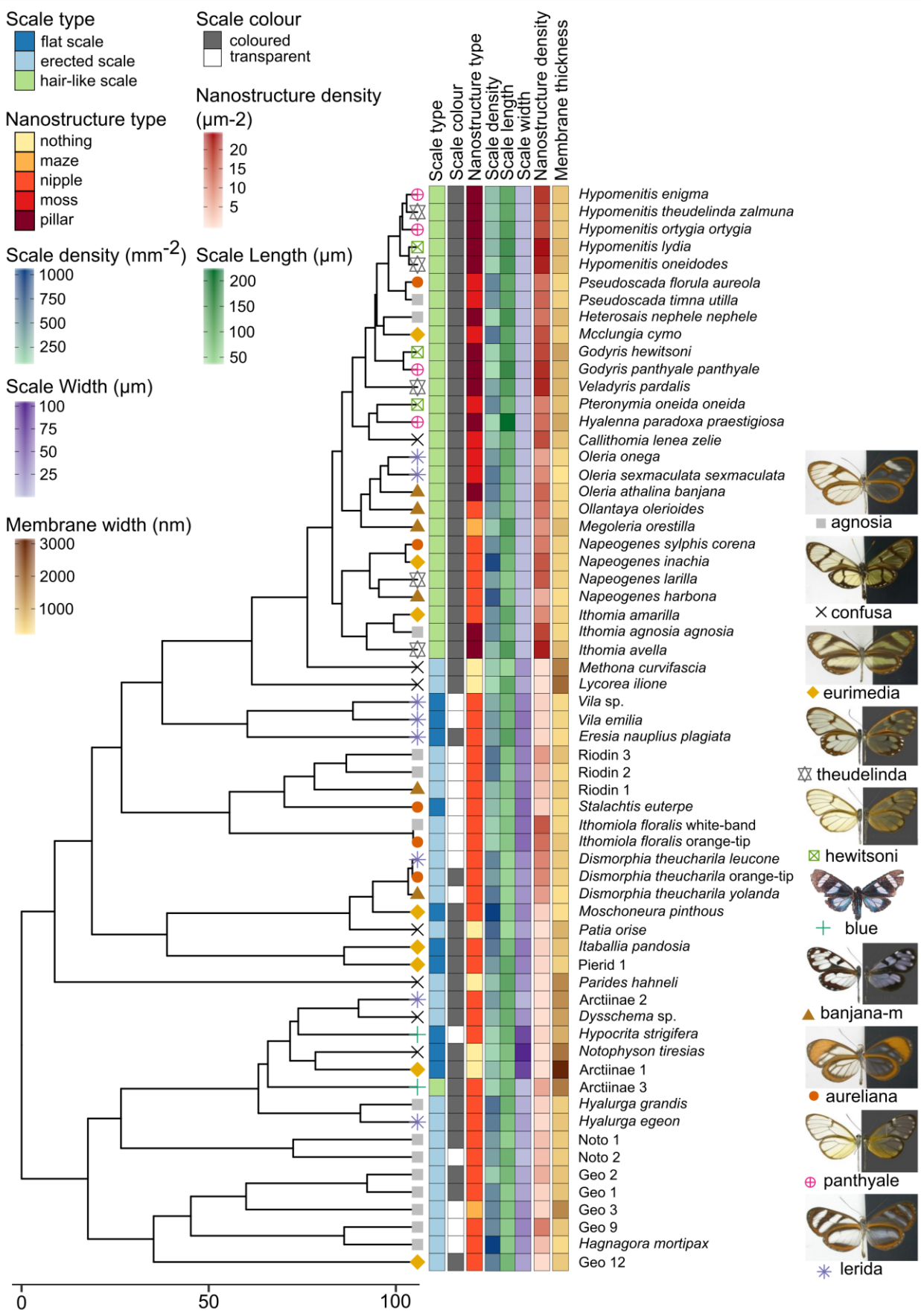

Figure 2. Phylogeny and distribution of traits along the phylogeny. Mimicry rings are represented by a symbol and a specimen is given as example for each mimicry ring.

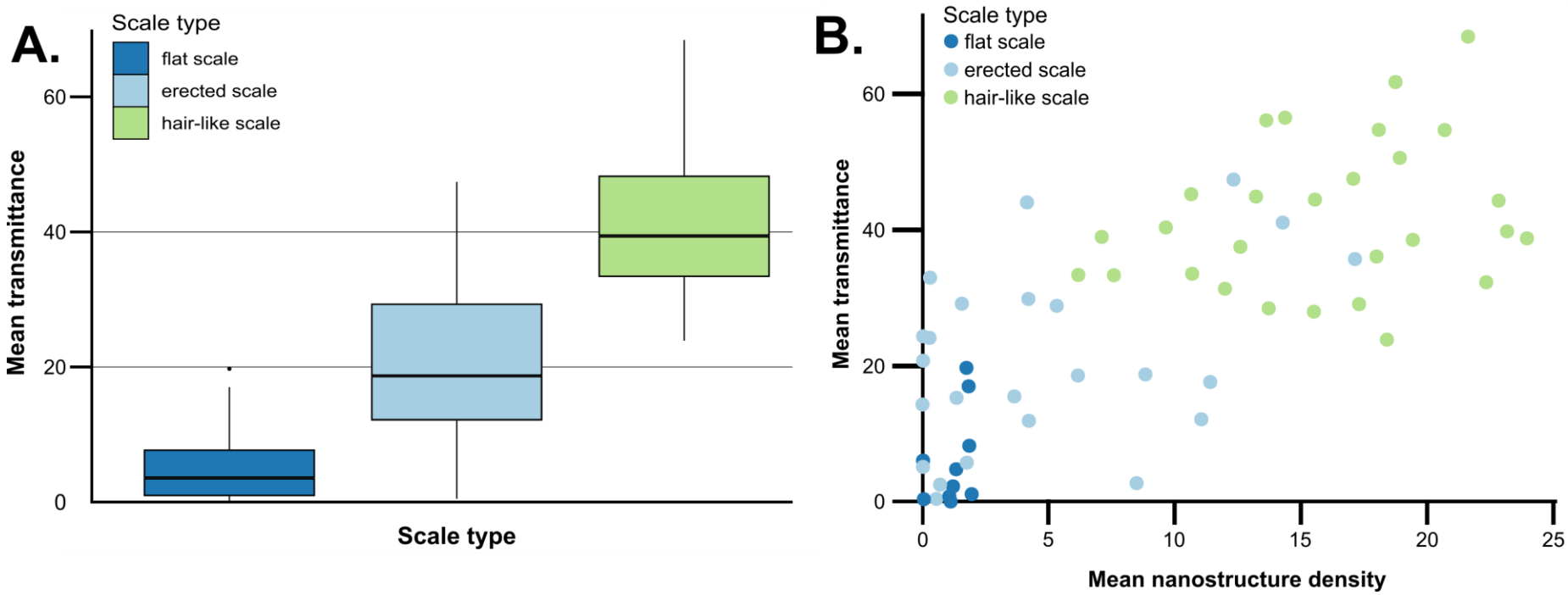

Figure 3. Link between mean transmittance and structural features.
A. Link between mean transmittance and scale type. B. Link between mean transmittance and nanostructure density and scale type.
NB. We considered the spot corresponding to the location of the SEM images for mean transmittance.